SK2 channels set a signalling hub bolstering CAF-triggered tumourigenic processes in pancreatic cancer

Raphael Rapetti-Mauss, Jérémy Nigri, Camille Berenguier, Pascal Finetti, Sarah Simha Tubiana, Bonnie Labrum, Benoit Allegrini, Bernard Pellissier, Georgios Efthymiou, Zainab Hussain, et al.

Title: SK2 channels set a signaling hub bolstering CAF-triggered Tumorigenic processes in pancreatic cancer

Authors: Raphael Rapetti-Mauss[1], Jérémy Nigri[2#], Camille Berenguier[1#], Pascal Finetti[2], Sarah-Simha Tubiana[2], Bonnie Labrum[1], Benoit Allegrini[1], Bernard Pellissier[1], Georgios Efthymiou[2], Zainab Hussain[2] Corinne Bousquet[4], Nelson Dusetti[2], François Bertucci[2], Hélène Guizouarn[1], Patricia Melnyk[3], Franck Borgese[1], Richard Tomasini[2*] and Olivier Soriani[1*].

[1]Inserm, CNRS, iBV, Université Côte d'Azur, Nice, France.

[2]Institut Paoli-Calmettes, Cancer Research Center of Marseille (CRCM), INSERM U1068, CNRS UMR7258, Aix-Marseille University, 13009 Marseille, France

[3]Univ. Lille, Inserm, CHU Lille, UMR-S1172 – LilNCog – Lille Neurosciences & Cognition, 59000 Lille, France.

[4]Cancer Research Center of Toulouse (CRCT), INSERM UMR 1037, University Toulouse III Paul Sabatier, ERL5294 CNRS, Toulouse, France.

* Co-last authors.

[#]: These authors contributed equally to this work.

Funding: The work described in this paper was supported by grants from the Fondation de France (RT: 00087538, Olivier Soriani: 00038330, 00059283) the French National Institute of Cancer (RT: INCA, PLBio13-134), La Ligue contre le Cancer (RRM: GB/MA/IQ-10607, GB/MA/CD/IQ-12187), Foundation ARC (RT: PJA20191209372, OS: PJA 2016 120 4740, PJA 2019 120 9546, RRM: PJA 2018 207701) and the Agence Nationale pour la Recherche (HG: ANR19-14-0049-01); JN was supported by Ministère de la Recherche and by Ligue contre le Cancer. CB was supported by the Fondation pour la Recherche Medicale. ST was supported by the French National Institute of Cancer (INCA, Pancreas 2017). BA was supported by the Ministère de la Recherche, de l'Enseignement Supérieur et de l'Innovation.

Acknowledgments: We thank the CRCM shared resources: Karim Sari and Regis Vitestelle for the PSEA animal facility, Michel Baccini, Bernard Chetrit and Eric Orlandi for informatical support, Bruno Olivier and Tahagan Titus for technical assistance. We also thank the Prism imagery facility of the iBV: Baptiste Monterroso and Sameh Ben Aicha. We are grateful to Véronique Rigot and Frédéric André for the kind gift of Gi9 antibody.

Abbreviations: PDAC, Pancreatic ductal adenocarcinoma; PCC, Pancreatic cancer cells; CAF, Cancer associated fibroblasts; ECM, Extra cellular matrix; Sig-1R, Sigma1 receptor (SigmaR1), EMT, Epithelial-to-Mesenchymal Transition

Corresponding authors:

Olivier Soriani: Inserm, CNRS, iBV, Université Côte d'Azur, Nice, France, Parc Valrose 28 Av. Valrose 06108 Nice. soriani@unice.fr

Raphael Rapetti-Mauss : Inserm, CNRS, iBV, Université Côte d'Azur, Nice, France, Parc Valrose 28 Av. Valrose 06108 Nice. Raphael.Rapetti-Mauss@univ-cotedazur.fr

Conflicts of interest: "The authors declare no potential conflicts of interest."

Abstract:

Objective: Intercellular communication within pancreatic ductal adenocarcinoma (PDAC) dramatically contributes to metastatic processes. The underlying mechanisms are poorly understood, resulting in a lack of targeted therapy to counteract stromal-induced cancer cell aggressiveness. Here we investigated whether ion channels, which remain understudied in cancer biology, contribute to intercellular communication in PDAC.

Design: We evaluated the effects of conditioned media from patient-derived cancer-associated-fibroblasts (CAF) on electrical features of pancreatic cancer cells (PCC). The molecular mechanisms were deciphered using a combination of electrophysiology, bioinformatics, molecular and biochemistry techniques in cell lines and human samples. An orthotropic mouse model where CAF and PCC were co-injected was used to evaluate tumor growth and metastasis dissemination. Pharmacological studies were carried out in the *Pdx1-Cre, Ink4a*$^{fl/fl}$ LSL-*Kras*^{G12D} (KIC^{pdx1}) mouse model.

Results: We report that the K^+ channel SK2 expressed in PCC is stimulated by CAF secreted cues (8,84 vs 2,49 pA/pF) promoting the phosphorylation of the channel through an integrin-EGFR-AKT axis. SK2 stimulation sets a positive feedback on the signaling pathway, increasing invasiveness in vitro (3 fold) and metastasis formation in vivo. The CAF-dependent formation of the signaling hub associating SK2 and AKT requires the Sig-1R chaperone. The pharmacological targeting of Sig-1R abolished CAF-induced activation of SK2, reduced tumor progression and extended the overall survival in mice (11,7 vs 9,5 weeks).

Conclusion: We establish a new paradigm in which an ion channel shifts the activation-level of a signaling pathway in response to stromal cues, opening a new therapeutic window targeting the formation of ion channel-dependent signaling hubs.

What is already known on this topic?

- PDAC remains a therapeutic dead-end partially due to the lack of targeted therapy.
- Intercellular communication between CAF and PCC largely contributes to PDAC aggressiveness.
- Sig-1R is an ion channel chaperon involved in the remodeling of electrical signature in various diseases.

What this study adds?

- SK2 channel, chaperoned by Sig-1R, is a mediator of the intercellular communication.
- SK2 activity is increased by direct AKT phosphorylation and stimulates a CAF-secretome-activated β-1-integrin-EGFR-AKT signaling hub.
- The inhibition of this signaling hub leads to a decrease in metastasis spreading and an increase in survival in PDAC mouse models.

How this study might affect research, practice or policy?

- Our findings highlight the SK2 channel as an original target to counteract stromal-induced cancer cell aggressiveness in PDAC that can be targeted through Sig-1R, a druggable chaperone.

Introduction:

Pancreatic Ductal Adenocarcinoma (PDAC) still represents a therapeutic dead-end. Despite a slight improvement of the overall survival, the global 5-year survival rate hardly progresses. As a hallmark of PDAC, the predominant intra-tumoral microenvironment – stroma - surrounding pancreatic cancer cells (PCC), is one of the main causes of treatment failure, emerging as a source of knowledge improvement and a niche for new therapeutic targets[1]. The stroma is composed of immune cells, blood and lymphatic vasculature, nerve fibers, and cancer-associated fibroblasts (CAF), all embedded in an abundant network of extracellular matrix (ECM) proteins. CAF participate in the dense fibrotic reaction in PDAC by sustaining ECM deposition, therefore largely contributing to PDAC aggressiveness. By interacting physically with PCC and through the secretion of soluble factors[2] or extracellular vesicles[3], CAF promote PCC invasive potency leading to metastasis formation[4] and exacerbate drug resistance[1]. CAF were widely described as tumor promoters. However, primary attempts to target the communication between the stroma and PCC revealed that non-specific targeting may enhance tumor development, suggesting a complex interplay between both compartments[1, 5, 6]. A finer strategy consists in focusing on the specific molecular mechanisms controlling the communication between CAF and PCC[7, 8], but the landscape remains incomplete. This situation illustrates the urgent need to understand the crosstalk between CAF and PCC, its impact on PCC abilities and PDAC evolution and investigate original drug targets.

SigmaR1 (Sig-1R) is a stress-activated and ligand-operated ion channel chaperone, controlling the electrical remodeling occurring in heart and brain diseases[9-12]. We showed in previous studies that Sig-1R induced electrical remodeling in cancers, promoting cell invasiveness[13, 14]. In the context of PDAC, we reasoned that 1) Sig-1R may participate in intercellular communication by promoting the remodeling of PCC's ion channels activity under the influence of CAF, and 2) Sig-1R regulated channels could be specifically targeted in PDAC using Sig-1R ligands.

A deep remodeling of the cells' electrical signature accompanies the development of numerous illnesses including cardiopathies, neurodegenerative diseases, inflammation and cancers[15, 16]. The role of ion channels has been appreciated in cancers, and growing evidence show their implication in cancer cell hallmarks by regulating Ca^{2+} homeostasis[15, 17], cell shape[18] and, nascently, signaling transduction pathways through the control of membrane potential (i.e. Wnt[19], KRAS[20]). However, the contribution of ion channels to intercellular communication within cancer tissues remains unknown.

Therefore, we aimed to understand the significance of CAF-secretome-induced ion channel regulation on PDAC progression. We show that CAF-secretome triggers the activation of the calcium-dependent K^+ channel SK2 thought its direct phosphorylation by AKT. SK2 is thenceforth included in a β1-integrin-EGFR-AKT signaling hub and sets a positive feedback loop amplifying tumorigenic processes. The activation and spatial dynamics of SK2 upon CAF-secretome exposure is dependent on Sig-1R. The pharmacological inhibition of Sig-1R abrogated CAF-induced metastatic spreading and improved overall survival. Altogether, these results demonstrate the unforeseen function for SK2 channel in tuning the intercellular communication between CAF and PCC and pave the way for potent therapeutic options in PDAC.

Materials and Methods

Cell Culture and CAF conditioned media production

HEK293T, PANC-1 and MiaPaCa-2 cell lines obtained from ATCC were maintained in Dulbecco's modified Eagle's medium with 10% fetal bovine serum, 100U/ml peniciline/streptomycin under 5% CO_2, 37°C in a humidified atmosphere. Cells were tested routinely for Mycoplasma contamination. CAF were obtained as previously described[3]. Briefly, CAF features were verified by immunofluorescence by a positive α-SMA staining and a negative pan-cytokeratin staining. We also further used a CD45, CD326 (Epcam), Pan-cytokeratin and CD31 FACS sorting to confirm that CAFs cultured are not immune, vascular or tumoral cells. CAFs were cultured in DMEM/F12, 10% FBS, 2 mmol/l l-glutamine, 1% antibiotic-antimycotic, and 0.5 mM sodium pyruvate and used between passages 4 and 10. When the monolayer reached 70-80% confluence, they were incubated in DMEM/F12 with 1% FBS (used as a control medium in experiments), and this conditioned media was collected every two days and stored at -20°C. Normal Human Fibroblasts (NHF) were isolated from healthy neonatal foreskins and cultured in DMEM, 10% FBS, 2 mmol/l l-glutamine, 1% antibiotic-antimycotic. Conditioned media was collected as described for CAFs.

Animal Studies:

For GEMM studies: Pdx1-Cre, $Ink4a^{fl/fl}$ LSL-$Kras^{G12D}$ (KIC^{pdx1}) male mice were obtained by crossing of the following strains: Pdx1-Cre, $Ink4a^{fl/fl}$, and LSL-$Kras^{G12D}$ mice provided by D. Melton (Harvard Stem Cell Institute, Cambridge, Massachusetts, USA), R. Depinho (Dana-Farber Cancer Institute, Boston, Massachusetts, USA), and T. Jacks (David H. Koch Institute for Integrative Cancer Research, Cambridge, Massachusetts, USA), respectively. PDAC-bearing 5- and 8-week-old mice were treated once a week with vehicle or 1(S) (0.1mg/injection/mouse) for survival follow-up until experimental endpoint: mice reaching sacrificing time or mice reaching physiological endpoints (cachexia criteria, limited movement, drinking or feeding of the mice). No exclusion has to be reported in all experiments as no mice

reached a criteria of exclusion such as a fight-related wound or the development of ear inflammation. To study final tumor volume, mice were euthanized at 9 weeks and tumors were weighed and fixed in 4% (wt/vol) formaldehyde for immunochemistry. For survival analyses, male mice were euthanized when they reached ethical clinical end points defined by our institutional guidelines and European animal protection law. For orthotopic tumor studies: the mice were anesthetized by isoflurane (Vetflurane; Virbac) inhalation in 30% air and 70% O_2. NMRI-Nude mice (Janvier Labs) under anesthesia were injected s.c. with 0.2 mg/kg buprenorphine (Vetergesic; Sogeval) and were administered lidocaine (Xylovet; Ceva) at 3.5 mg/kg by infiltration in the abdominal cavity. A first incision was made at the top left of the abdomen and a second at the peritoneum to reach the pancreas. PANC ShRD/ PANC ShSig-1R/ PANC ShSK2 cells alone (500,000 cells) or plus CAF (1,500,000 cells) contained in 40µL of PBS were injected into the pancreas. The abdominal musculature was then closed with 4-0 sutures and the external skin with inverted stitches. The mice were euthanized 8 weeks later. The pancreas was removed and weighed, the liver removed and analyzed for macroscopic metastases. These organs were fixed in 4% formaldehyde for immunochemistry. Liver metastases were confirmed and counted per mouse using H&E staining.

For all experiments, sample size was predicted following a Mann-Whitney statistical approach involving power calculation of 0.8 with a FDR of 0.05. A minimum number of 7 mice per group was predicted as able to reach significance. Bonferroni post-hoc test was used for multiples test comparison (two variance with time and/or treatment). Experimental technicians were proceeding with injections while personnel related to mice follow-up worked in a blinded approach. All animal care and experimental procedures were performed in agreement with the Animal Ethics Committee of Marseille and the French ministry of research and innovation under the reference Apafis#16998-2018100814458519.

Gene expression analysis of human PDAC samples

We gathered clinicopathological and gene expression data of clinical pancreatic samples from 16 publicly available data sets (Table S2). Data were collected from ArrayExpress, EGA, National Center for Biotechnology Information (NCBI)/Genbank GEO, and TCGA databases and had been generated using DNA microarrays (Affymetrix, Agilent, Illumina) and RNA-seq (Illumina). The pooled data set contained 1,017 samples, including 925 primary PC samples, and 92 metastases. The study was approved by our institutional board.

Statistical analysis

Each experiment was repeated independently at least three times. Results are presented as median with interquartile range unless stated otherwise. For comparison between two quantitative variables, we used the Mann-Whitney test. When more than two variables were compared, Kruskal-Wallis tests were used followed by a Dunn's post-test, unless stated otherwise. For comparison between fold change a one sample t test was applied. Log-Rank (Mantel-Cox) test was used to evaluate mice survival. Analyses were performed using either GraphPad Prism V.8.0.1 or R software. A p value <0.05 was considered statistically significant.

Additional materials and methods are provided in the Supplementary Material.

Results:

Secreted cues from CAF stimulate SK2 in pancreatic cancer cells.

To determine whether Sig-1R participates in electrical remodeling in PDAC, we recorded ion channel activity in PCC (i.e. PANC-1 and MiaPaCa-2) where Sig-1R expression was silenced by short hairpin (sh) RNA. Abrogation of Sig-1R expression led to the inhibition of a K^+ conductance exhibiting an inward rectification typical of small conductance calcium-dependent K^+ channels. Further pharmacological and molecular analysis revealed that the current was suppressed by the SK-channels inhibitor Apamin, the SK2-specific inhibitor Leiurotoxin-1 Dab-7 (Fig. 1A, B), and by molecular silencing of SK2 channel (Fig. S1A, S1B). Interestingly, immunostaining of human PDAC specimens confirmed that Sig-1R and SK2 are effectively expressed in PDAC (Fig. 1C). To investigate the influence of secreted factors from CAF on

SK2 channel in PCC, we have generated a conditioned media using human primary CAF obtained from PDAC patients (CAF-CM; Fig. 2A). CAF subtyping was investigated by flux cytometry using a panel of markers including iCAF, myCAF and apCAF markers as well as more transverse markers recently identified such as CD105. As shown in Figure S2, the CAF cultured for this study were mainly Podoplanin^{high}, CD105^{high}, PDGFRβ^{high}, FAP^{high} and αSMA^{low}. We observed that PANC-1 incubation with CAF-CM (overnight) increased the Dab7-sensitive current (ISK2, Fig. 2B), an effect abolished by the molecular silencing of SK2 using ShRNA or Crispr/Cas9 technology (Fig. 2B, C). Importantly, CM harvested from Normal Human Fibroblasts (NHF cells) failed to stimulate the current, indicating that the effect is specific to CAF-secretome (Fig. 2D). Furthermore, boiled CAF-CM had no impact on the current, ruling out any involvement of secreted metabolites (Fig. S3). The CAF-CM-mediated activation of ISK2 was dependent on Sig-1R since this effect was abolished by the molecular silencing of Sig-1R and rescued by the expression of C-myc Sig-1R in the shSig-1R cell line (Fig. 2E, F). Since Sig-1R modulates ion channel function through protein-protein associations[21, 22], we asked whether Sig-1R and SK2 could form complexes upon CAF-CM exposure using proximity ligation assay (PLA). In PANC-1 challenged with CAF-CM, the interaction between SK2 and Sig-1R was significantly increased (Fig. 2G). Altogether, these results show that CAF-CM triggers SK2 in a Sig-1R-dependent manner in PCC.

CAF-secretome activates SK2 through an Integrin-EGFR-AKT pathway.

To understand how CAF-CM stimulates SK2 current (ISK2), we examined the activation state of a subset of signaling kinases in PANC-1 using a phosphokinase array. We observed that the most robustly CAF-CM-activated kinases were associated to two main signaling clusters: one associated to the EGFR-AKT axis (EGFR, Src, AKT, Wnk1, AMPKa1, mTor, CREB) and the other to integrin signaling (FAK-Src) (Fig. 3A). We thus evaluated the effects of treatments altering each of these pathways on SK2 activity. EGF treatment induced a significant increase in ISK2, which was dependent on Sig-1R (Fig. 3B). Accordingly, the EGFR inhibitor Erlotinib and the AKT inhibitor DEBC both suppressed the CAF-CM-induced ISK2 (Fig. 3C, D). These

data indicate that CAF-CM-induced SK2 stimulation depends on EGFR-associated signaling. Given that CAF-CM treatment triggered FAK in the phosphokinase array, we tested the effect of fibronectin (FN), an element of the stroma that activates FAK via the α5β1-integrin in PCC[23]. FN mimicked the effects of CAF-CM on ISK2 (Fig. 3E). Incubation of cells with a functional anti-β1-integrin antibody abolished the CAF-CM-induced increase in ISK2 (Fig. 3E), further demonstrating that CAF-CM-dependent SK2 activation requires integrin/FAK transduction. To confirm the functional links between the different partners at the molecular level, we performed PLA experiments and observed that SK2 associates with EGFR, the β1-integrin subunit and AKT. These associations were promoted by CAF-CM treatment and required Sig-1R, as shown by experiments using ShSig-1R PANC-1 cells (Fig. 3F). These results reveal that SK2 activity is modulated by a CAF-CM stimulated signaling hub, stabilized by Sig-1R. We therefore looked for the presence of EGF and FN in CAF-CM. Surprisingly, we were able to detect EGF neither in a proteomic analysis of the CAF-CM nor using a sensible EGF ELISA test (Fig. S4A). Note that EGF could not be detected in the culture media of PANC-1 cells cultivated with control medium or CAF-CM (Fig. S4B). In support of this, neither EGF, nor other EGFR ligands (i.e. TGFα, HBEGF, BTC, AREG, EREG and EPGN) could be detected in the proteomic analysis. By contrast, the analysis revealed that FN is one of the most abundant components of CAF secretome (Table S1), a result confirmed by an immune-dot blot assay (Fig. 3G). Interestingly, the treatment of PANC-1 with FN induced the association between AKT and SK2, mimicking the effects of CAF-CM (Fig. 3H). Since β1-integrin can form complex with other α-sub-unit integrins, we next ask whether other components of the CAF-CM could participate in the stimulation of the current. Proteomic analysis of CAF-CM revealed the presence of Collagen I, a ligand of the α2β1 integrin which is expressed in PDAC cells and participates in PDAC cell phenotype[24, 25]. Interestingly, the specific α2-integrin blocking antibody Gi9 significantly reduced CAF-CM-induced stimulation of SK2 current (Fig. S5) while Collagen I stimulated AKT/SK2 association (Fig. 3H). Finally, these results are globally reinforced by the colocalization between Sig-1R/SK2 and p-AKT observed by immunohistochemistry from PDAC patient samples (Fig. 3I). Altogether, these data indicate that components secreted by

CAF-CM that stimulate β1-dependent integrins such as FN or Collagen I potentially activate SK2 via the same signaling hub.

SK2 is a pivotal regulator of the AKT signaling pathway

Since the activation of ISK2 by the CAF-CM depends on AKT, we hypothesized that SK2 could be a target protein of AKT. Using sequence alignment, we identified 3 residues (S562, S568, S569) corresponding to the AKT consensus phosphorylation motif in the SK2 sequence (RxRxxST). Strikingly, this motif was conserved in SK2 orthologs from different species (Fig. 4A), but was absent in SK1, SK3 and SK4 sequences, suggesting a specificity of AKT for SK2 among the SK family. Co-expression of SK2 and a constitutively active form of AKT (Myr-AKT) in HEK293 cells resulted in a significant increase in SK2 current compared to the control condition. Co-expression of Myr-AKT with SK2 carrying a triple phospho-resistant mutation (S562A, S568A, S569A) failed to increase channel activity, suggesting that AKT stimulates ISK2 by phosphorylating the channel on at least one of the three phosphorylation sites (Fig. 4B). To further demonstrate that SK2 is a target of AKT we used a phospho-specific antibody that recognizes the AKT phosphorylation consensus motif. Co-immunoprecipitation experiments show that Myr-AKT indeed phosphorylated the WT SK2 channel but failed to phosphorylate the triple phospho-resistant mutant of SK2 (Fig. 4C). Patch clamp recording in HEK293 transfected with SK2 revealed that S568 and S569 residues were phosphorylated by AKT activation upon CAF-CM exposure (Fig. 4D), demonstrating that SK2 is a specific target of AKT. To further understand how AKT phosphorylation impacts the regulation of the channel we used the phospho-mimetic mutation S568D, which abolished the calcium sensitivity of SK2 (Fig. 4E). Moreover, upon CAF-CM treatment, the activity of SK2 in PANC-1 cells did not change after decreasing the intracellular calcium concentration from 1µM to 0.1µM (Fig. S6), indicating that the AKT-dependent phosphorylation of SK2 following CAF-CM exposure renders the channel independent on intracellular calcium concentration. However, at this stage, the functional consequences of AKT-dependent SK2 activation on cancer cell behavior remained an open question. Therefore, we looked for the signaling pathways regulated by

CAF-CM-mediated activation of SK2. We measured the phosphorylation levels of the individual kinases monitored with a phosphokinase array, in control and SK2-silenced PANC-1 cells challenged with CAF-CM. We observed that the silencing of SK2 blocked CAF-CM-induced phosphorylation of 8 kinases among the 12 that were CAF-CM sensitive (Fig. 4F). Only kinases showing a significant reduction in their phosphorylation level in both SK2-silenced cell lines (i.e. ShSK2 and Crispr-Cas9 KO-SK2 PANC-1 cell lines) were considered and we found that AKT (S473), Yes (Y426), Src (Y419), FAK (Y397), EGFR (Y1086), WnK1 (T60), AMPKa1 (T183) and GSK3β (S21/S9) were activated in a SK2-dependent manner (Fig. 4G). Since these kinases belong to the EGFR-AKT-β1-integrin-associated signalosomes targeting the channel, these results suggest that activating SK2 sets a positive feedback loop on this signaling axis which is largely involved in cancer physiopathology[26].

SK2 drives PCC aggressiveness in response to CAF secretome in vitro and in vivo

To test whether SK2 stimulation could favor PCC aggressiveness, we first evaluated the expression of adherent junctions (AJ) markers since loss of AJ coincides with loss of epithelial features and increases invasive phenotypes[27]. Using PCC ShRD as controls, we confirmed that CAF-CM provoked a decrease in E-cadherin, β-catenin, and P-120 catenin levels- three AJ markers - (Fig. 5A). The molecular silencing of SK2 (or Sig-1R) abolished the effect of CAF-CM on AJ markers (Fig. 5A; Fig. S7A, B). To further explore this idea, we performed FACS analyses using an epithelial marker (Epcam / CD326) and a mesenchymal marker classically activated following Epithelial-to-Mesenchymal Transition - EMT (CD106)[28]. The addition of CAF-CM on control PCC (ShRD) enhances their EMT phenotype whereas EMT reprogramming is lost in PCC depleted for Sig-1R or SK2 (Fig. 5B). As a main functional consequence of epithelial markers loss and EMT reprogramming, we then explored invasive potency of PANC-1. As expected, CAF-CM exposure significantly enhanced PCC invasive abilities (Fig. 5C). Consistent with epithelial and EMT markers data, the enhanced invasive properties driven by CAF-CM were lost in SK2- or Sig-1R-deficient PCC (Fig. 5C). Moreover, when grown in 3D condition, CAF-CM increased the formation of protrusions in ShRD control

cells, as shown by F-Actin immunofluoresence (Fig. 5D, left panel) and Filopodia density measurement (Fig. 5D, right panel), but not in SK2- or Sig-1R-deficient PCC (Fig. 5D). Interestingly, Sig1R or SK2 silencing altered neither cell growth, nor cell survival, but strongly decreased cell migration (Fig. S8A, B, and C). Moreover, using a public PDAC patient database ([Dataset] oncoR2 platform; http://r2.amc.nl; n=130)[29], we revealed that the expression of both SK2 and Sig-1R are negatively correlated to AJ markers expression (Fig. S9). Reinforcing this result, co-staining between SK2 or Sig-1R and an epithelial (Pan Cytokeratin) or a mesenchymal (α-SMA) marker in PDAC patient samples showed that Sig-1R and SK2 expression patterns are strictly limited to pan cytokeratin-expressing cells and co-localize with α-SMA (Fig. 5E, F). These results suggest that Sig-1R and SK2 are expressed in epithelial cancer cells that have undergone EMT, a process favored under CAF crosstalk condition, and reported to impact metastatic burden[30]. To further challenge this hypothesis, we orthotopically transplanted either ShRD, ShSK2 or ShSig-1R PANC-1 cells in presence, or not, of CAF into the pancreas of NMRI-nude mice (Fig. 5G-M). As expected, co-injection of ShRD PCC and CAF revealed an increase in tumor weight (Fig. 5H, L), development of liver metastasis (Fig. 5I, M) and EMT reprogramming of epithelial cells (Fig. 5J). Interestingly, silencing of SK2 or Sig-1R in PCC abrogated CAF-induced increase in tumor weight (Fig. 5H and L), metastasis formation (Fig. 5I, M) and EMT (Pan CK/α-SMA co-labelling, Fig. 5J) corroborating our hypothesis. Of interest, we controlled the presence of CAFs by the time of euthanasia in co-injected mice by identifying cells only labelled by αSMA staining as a CAF marker, and could validate their presence, consistently with previous publications using CAF/tumor cell orthotopic co-injections[3] (Fig. S10). Altogether, these results support the idea that SK2 constitutes an essential signal transducer for the intercellular communication between CAF and PCC, bolstering PCC aggressiveness, tumorigenesis, and metastasis development.

A Sig-1R ligand inhibits SK2 activity and improves survival in vivo

Considering that the coupling between SK2 and AKT relies on Sig-1R, we sought to test whether targeting SK2 via Sig-1R in PDAC would be a valuable therapeutic strategy. Sig-1R

ligands are synthetic small molecules that modify the coupling of Sig-1R with its partners including ion channels[10, 13]. Compound **1(S)** is a Sig-1R ligand exhibiting nanomolar affinity for Sig-1R (IC_{50} = 3.9 nM), high Sig-2R/Sig-1R selectivity (greater than 120) and very low cytotoxicity (selectivity index, ratio CC_{50}/IC_{50}, greater than 50 000)[31]. We first validated in vitro that **1(S)** abolished the CAF-CM mediated activation of SK2 and prevented the association of SK2 and AKT by patch-clamp (Fig. 6A) and PLA experiments (Fig. 6B). Proliferation and viability assays, on control Panc-1 cells or cells silenced for Sig1R or SK2, demonstrated that **1(S)** treatment does not exhibit any effect on these parameters (Fig. S8A, B). We next evaluated the effect of **1(S)** in an endogenous PDAC mice model (KIC^{pdx1})[32]. By using a first protocol treating the KIC^{pdx1} mice at 5 weeks old, before the onset of PDAC (Fig. 6C), we observed that **1(S)** treatment significantly delayed tumor progression and extended the overall survival. The median survival time of KIC^{pdx1} non-treated animals was 9.5 weeks, whereas median survival of KIC^{pdx1}-**1(S)** treated mice was 11,7 weeks (Fig. 6D). This data was confirmed on a similar treatment protocol combined to an end-point study at 9 weeks of age (Fig. 6E), representing the median survival of KIC^{pdx1} non-treated mice, validating that **1(S)** treatment delayed tumor progression. Indeed, as shown in Figure 6F, in **1(S)** treated KIC^{pdx1} mice, the pancreatic tumor/body mass ratio showed a drastic reduction of 69% compared to non-treated ones, decreasing from 0.065 for KIC^{pdx1}non-treated mice to 0.021 for **1(S)** treated KIC^{pdx1} mice. Histological examination of pancreas from **1(S)** treated KIC^{pdx1} mice revealed an almost lack of malignant lesions contrasting with pancreas of non-treated KIC^{pdx1} mice exhibiting typical PDAC development (Fig. 6G). In addition, **1(S)**-treated mice exhibited a lower number of EMT-reprogramming epithelial cells (Pan-CK/αSMA co-staining, Fig. 6H) and a lower ECM density reflecting a decreased desmoplasia in treated animals (trichrome labelling, Fig. 6I, J, K). Furthermore, we have tested the efficiency of **1(S)** treatment on PDAC evolution using an alternative protocol starting the treatment of KIC^{pdx1} mice at 8 weeks of age (Fig. 6L), when PDAC has already developed. Using this experimental design, we confirmed that **1(S)** treatment significantly extended the overall survival. Indeed, the median survival time of KIC^{pdx1} non-treated animals was 8,8 weeks, whereas median survival of KIC^{pdx1}-**1(S)** treated mice was

11 weeks (Fig. 6M). Together, these results illustrate that SK2 inhibition via Sig-1R ligand delays PDAC development and significantly extends survival, supporting **1(S)** as a valuable therapeutic option to treat PDAC.

SK2 and Sig-1R expression in PDAC correlates with metastatic phenotype

To characterize the expression of Sig-1R in human PDAC, we interrogated publicly available gene expression datasets from 1,017 patients with pancreatic carcinoma ([Dataset] Table S2). First, we found that SIGMAR1 (encoding Sig-1R: Fig. 7A), and KCNN2 genes (encoding SK2: Fig. 7B), were more expressed in metastases than in primary tumors, and preferentially in liver metastases. Second, in an analysis limited to the 925 primary cancers, SIGMAR1 expression, assessed as binary value (cut-off equal to median expression level), was not associated with patients' age and gender, pathological tumor type and grade, and American Joint Committee on Cancer (AJCC) stage (Table S3). Regarding the molecular subtypes (Table S4), no correlation existed between SIGMAR1 expression (Fig. 7C) and the [Dataset] Bailey's classification[33] (pancreatic progenitor, immunogenic, squamous), the [Dataset] Collisson's classification[34] (quasi-mesenchymal, classical), and the [Dataset] Moffitt's classification[35] (basal, classical). By contrast, KCNN2 expression was higher in the squamous Bailey's subtype, the quasi-mesenchymal Collisson's subtype, and the basal Moffitt's tumor subtype (Fig. 7D). These results revealed higher gene expression of SK2 and Sig-1R in metastases versus primary cancers, and higher expression of SK2 in aggressive molecular subtypes.

Discussion

The stromal compartment participates in PDAC onset, development, and aggressiveness. However, recent studies refined the variety of stromal cellular components such as CAF, and their abilities to potentially support or restrain PDAC progression[1, 5, 6, 36, 37]. This knowledge highlighted the necessity to precisely identify and target stromal cues and mechanisms that underlie the pro-tumoral intercellular communication between CAF and pancreatic cancer cells (PCC). Herein, the potassium channel SK2 was found to mediate intercellular communication between PCC and CAF by amplifying an EGFR-AKT axis upon CAF-secretome-stimulation, promoting metastatic spreading and poor survival in pancreatic cancer. The association between SK2 and its partners is controlled by the ligand-modulated ion channel chaperone Sig-1R which can be pharmacologically targeted to reduce CAF-induced tumorigenic processes particularly metastasis.

Interestingly, we have shown that exposure to CAF-CM induces an increase in SK2 current in PCC, suggesting that this channel participates in the CAF-secretome-mediated intercellular communication in PDAC. Several secreted factors from CAF, within PDAC stroma, like growth factors[38], cytokines[7], and lipids[8], were shown to mediate paracrine communication that stimulate PCC aggressive features. Our data show that the CAF-CM-mediated activation of SK2 was dependent on EGFR activity. Indeed, this effect was mimicked by EGF treatment and completely abolished using Erlotinib. Surprisingly, we have been unable to detect EGF in the CAF-secretome. Looking deeper, we found that fibronectin and collagen I, two major components of CAF-CM, activate a β-1-Integrin/EGFR/AKT signaling axis that increases SK2 activity in PCC. The abundant presence of fibronectin and Collagen I has been revealed in stromal PDAC patients and mouse models samples[37, 39] as well as in the secretome obtained from human primary CAF[40]. Several studies have demonstrated that fibronectin and Collagen I contribute to PCC aggressiveness, survival and chemoresistance[24, 41]. These results strongly suggest a transactivation mechanism of EGFR, that has been previously reported as integrin- and FAK-related in PDAC[26, 42]. Our data support the idea that secretion of ECM components

within PDAC microenvironment would be a key mediator in the CAF-stimulated formation of a signaling hub including SK2, the β1-integrin, EGFR and AKT, that finely tunes the activity level of the downstream intracellular signaling pathway supporting PDAC development and metastasis formation.

SK2 seems to have a pivotal role in this signaling hub. Indeed, we reveal that the channel is a direct target of AKT, since we identified an AKT-specific motif within the channel sequence containing 2 serine residues that are phosphorylated upon CAF-CM treatment (S568 and S569), both being necessary to mediate CAF-CM induced SK2 activity. We also found that the AKT specific phosphorylation site in SK2 is highly conserved among species, but lacks in the other members of the SK channel family (i.e. SK1, SK3 and SK4), reinforcing the idea of a functional and specific coupling between SK2 and AKT-dependent pathways. Interestingly, we found that the channel phosphorylation by AKT stimulated the current by increasing its activity at sub-threshold intracellular Ca^{2+} concentrations. These findings highlight an unexpected direct up-regulation of SK2 activity by AKT.

EGFR activation is associated to AKT phosphorylation in PDAC[42, 43] and the EGFR-PI3K-AKT signaling axis is one of the main signaling pathways involved in PDAC progression[44]. Therefore, we reasoned that the AKT-dependent activation of SK2 could be crucial in the Integrin-EGFR-AKT axis. Our results, showing that SK2 silencing reduced CAF-dependent signalization, suggest that without a functional channel, PCC remain in a sub-threshold state that prevents the metastatic process despite stimulation by CAF. Accordingly, SK2 inhibition reversed the capacity of CAF to induce aggressiveness, and stabilized cells in an epithelial state. Thus, these data provide arguments to propose that SK2 sets an activation threshold that switches PCC from an epithelial state when SK2 activity is low, to a pro-invasive state when channel activity is high, underlined by EMT-reprogramming. To support this model, SK2 silencing decreased CAF-induced cell invasiveness, tumor growth and metastasis formation in vivo. These results correlate with our investigation of human PDAC expression datasets revealing that SK2 expression is increased in liver metastasis compared to primary tumors,

and that SK2 expression is significantly higher in the more aggressive subtype of PDAC cancer cells. Thus, these results highlighted SK2 as an ion channel playing a pivotal role in transducing extracellular signals from the tumor microenvironment onto intracellular activation of oncogenic signaling pathways in PCC.

Currently, the therapeutic armamentarium to treat PDAC is restricted and poorly efficient. A better understanding of the molecular components that participate in intercellular communication suggests novel strategies for treating PDAC. Here we have shown that the ligand-modulated chaperone Sig-1R was required for the activation of SK2 current and the assembly of the SK2-AKT-β1-integrin-EGFR signaling hub upon PCC stimulation by CAF. This observation is in line with previous studies showing that Sig-1R contributes to electrical remodeling by promoting channel/channel or channel/receptor associations[13, 14, 45]. Interestingly, Sig-1R silencing recapitulates the effects of SK2 silencing in vitro and in vivo.

On another hand, we have demonstrated that PCC treatment with the selective Sig-1R ligand **1(S)** abolished CAF-CM-driven association between SK2 and AKT, underlying current inhibition. More importantly, pharmacological inhibition of Sig-1R was efficient in vivo as mouse models of PDAC treated with **1(S)** dramatically delayed tumor development, reduced metastasis onset and extended survival. Although stromal ablation for PDAC treatment remains controversial, our results suggest a potential therapeutic opportunity by targeting an ion channel-dependent signaling hub through its regulator, Sig-1R, a druggable ion channel chaperone[9, 46], to reduce stromal-induced PDAC aggressiveness (Fig. 8). Because Sig-1R activity is stimulated by stress in diseased tissues[47], the use of Sig-1R ligands should specifically target SK2 in tumors but not in brain or heart. In support of this, a recent study revealed that Sig-1R ligands modulate ion channels in cardiomyocytes from long QT syndrome patients, but not in cardiomyocytes from isogenic controls[12].

Prospective studies combining Sig-1R targeting with other therapeutic approaches, as chemotherapeutics agents, are necessary to evaluate their potential as long-term durable anti-PDAC response. Further evaluation of the Sig-1R/SK2/CAF crosstalk in other solid tumors

would open new avenues to consider channel and chaperone proteins targeting as anti-cancer therapeutic options.

Figures legends

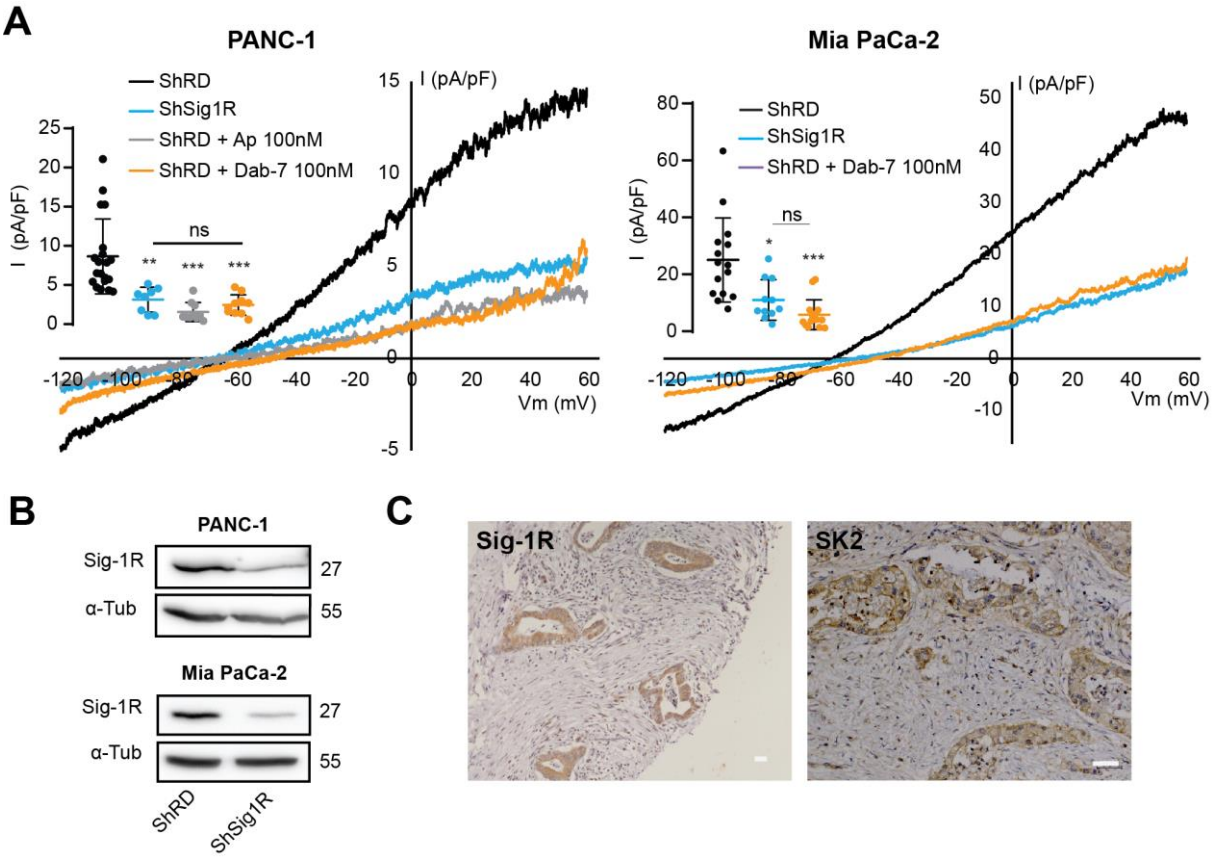

Figure 1: Sig-1R regulates a potassium current in Pancreatic cancer cells. *(A)* Patch clamp recordings of current elicited in control (ShRD PANC-1, n=20; MiaPaCa-2, n=15) or Sig-1R-silenced (ShSig-1R PANC-1, n=8; MiaPaCa-2, n=11) PCC, in the absence or presence of SK2 channel inhibitors apamin (Ap.100nM, PANC-1, n=10) or leiurotoxin-1 Dab-7 (Dab-7, 100nM; PANC-1, n=10; MiaPaCa-2, n=15). *(B)* Western blot analysis of shRNA-mediated Sig-1R silencing efficiency in PANC-1 and MiaPaCa-2 cells. *(C)* Representative immuno-histochemistry staining for Sig-1R and SK2 expression in PDAC patient samples. Scale bar, 50 µm. (*P< 0,05, **P< 0,01; ***P< 0,001; ns: not significant).

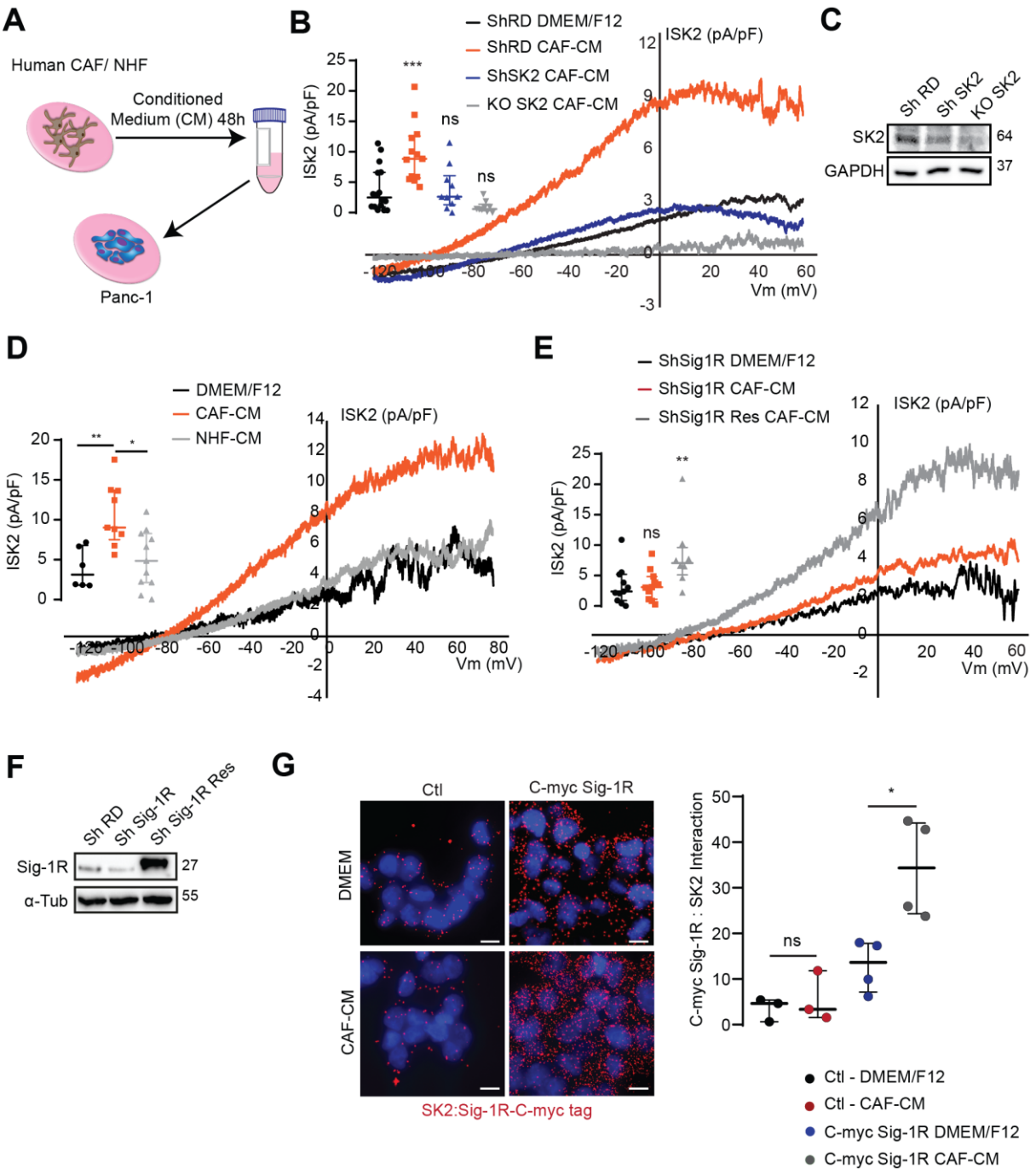

Figure 2: Secreted cues from CAF derived from PDAC patients stimulate SK2 channel. *(A)* Schematic representation of conditioned medium production from patients-derived CAF (CAF-CM) and Normal Human Fibroblast (NHF-CM). *(B)* Patch clamp recordings of Dab-7-sensitive current (ISK2) from the following conditions: ShRD PANC-1 cells exposed to 1%-FBS DMEM/F12 (negative control - DMEM/F12, n=16) or ShRD PANC-1 cells (n=13), ShSK2 PANC-1 cells (n=10), and KO-SK2 PANC-1 cells (n= 9) exposed to CAF-CM overnight. *(C)* Western blot analysis of shRNA (ShSK2) and Crispr/Cas9-mediated (KO-SK2) SK2 silencing

efficiency in PANC-1 cells. *(D)* Patch clamp recordings of Dab-7-sensitive current (ISK2) from the following conditions: ShRD PANC-1 cells exposed to 1%-FBS DMEM/F12 (negative control - DMEM/F12, n=6) or ShRD PANC-1 cells exposed to either CAF-CM (n=9) or NHF-CM (n=11) overnight. *(E)* Patch clamp recordings of Dab-7-sensitive current (ISK2) from the following conditions: ShSig-1R PANC-1 cells exposed to 1%-FBS DMEM/F12 (negative control - DMEM/F12, n=11), or ShSig-1R PANC-1 cells (n=11) and ShSig-1R PANC-1 cells where Sig-1R has been rescued using a C-myc Sig-1R construct (ShSig-1R Res n= 8), exposed to CAF-CM overnight. *(F)* Western blot analysis of Sig-1R protein expression, showing the rescue of Sig-1R in ShSig1R-Res PANC-1 cells. *(G)* PLA analysis of the interaction between SK2 and C-myc-Sig-1R in control (Ctl) or C-myc Sig-1R PANC-1 cells treated with DMEM/F12 or CAF-CM; n=3-4; Bar: 10µm. (*P< 0,05, **P< 0,01; ***P< 0,001; ns: not significant).

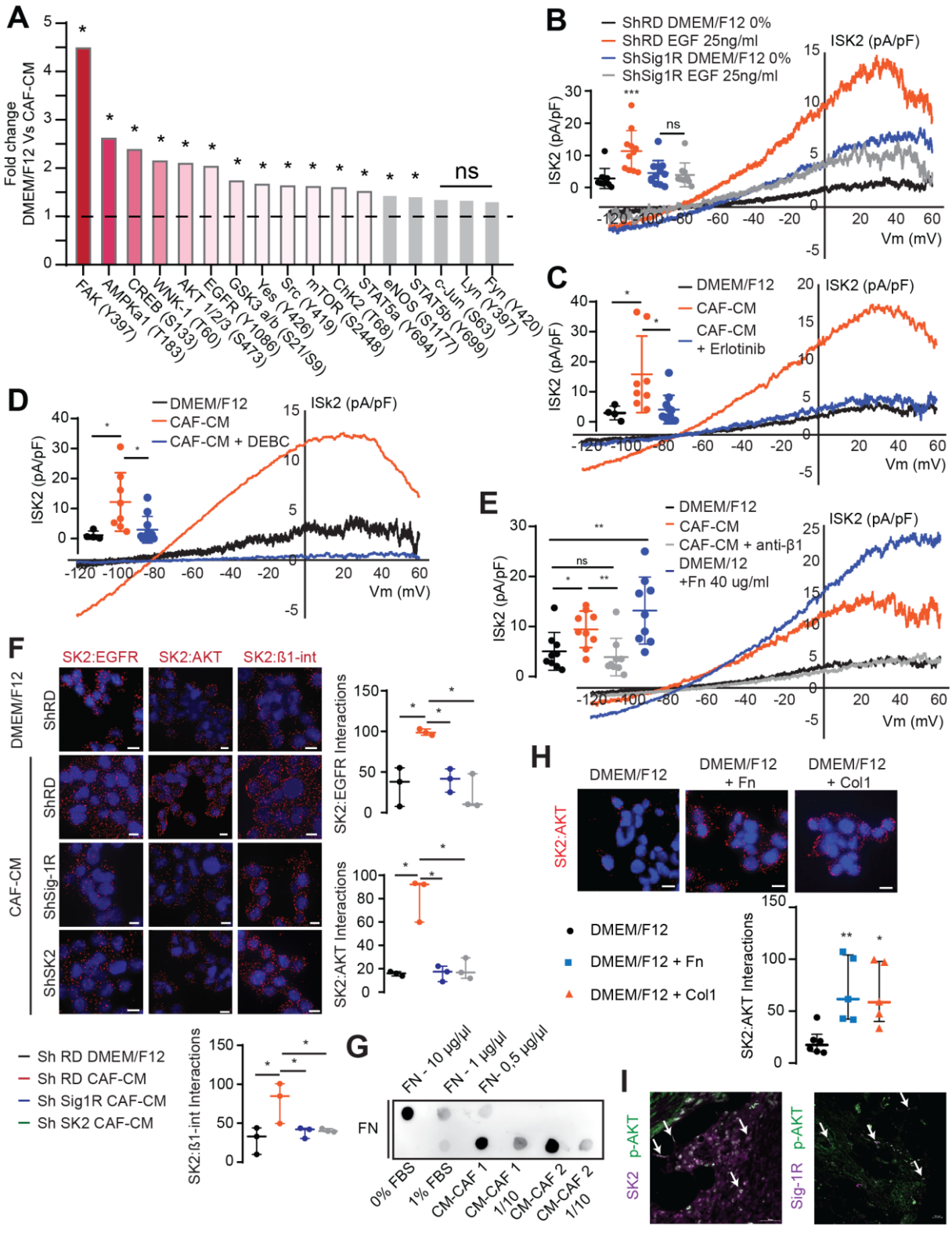

Figure 3: Fibronectin from CAF secretome activates SK2 through an Integrin/EGFR-PI3K-AKT pathway. *(A)* Bar graph showing fold change in phosphorylation levels of a set of signaling proteins upon overnight exposure of PANC-1 cells to CAF-CM relative to control

(DMEM/F12). Experiments were performed in experimental duplicates (n=3, *P< 0,05). *(B)* ISK2 was recorded in ShRD and ShSig-1R PANC-1 cells, treated overnight with 0%-FBS DMEM/F12 (ShRD, n=10; ShSig-1R, n=12) or 0%-FBS DMEM/F12 supplemented with 25 ng/ml EGF (ShRD, n=11; ShSig-1R, n=10). *(C-E)* Patch clamp recording of ISK2 in PANC-1 cells exposed overnight to *(C)* control medium (n=4) or CAF-CM (n=8) pretreated or not 1hour with 10µM erlotinib before adding CAF-CM (n=12); *(D)* control medium (n=4) or CAF-CM (n=8) treated or not 10min before recording with 10µM DEBC (n=11); *(E)* control medium (n=9), CAF-CM (n=9), Fibronectin (Fn 40µg/ml; n=9), or CAF-CM treated on ice with a functional antibody against the β1-integrin 30min before recording (10µg/µl; n=9). *(F)* PLA analysis of the interaction between SK2/EGFR, SK2/AKT and SK2/β1-integrin in ShRD, ShSig-1R or ShSK2 PANC-1 cells treated overnight with control medium or CAF-CM, (n= 3); Scale Bar: 10µm. *(G)* Dot blot assay showing the presence of Fibronectin (FN) in different conditions: DMEM/F12 0%-FBS, or 1%-FBS, and in 2 different batch of CAF-CM. *(H)* PLA analysis of the interaction between SK2 and AKT in PANC-1 cells, treated overnight with control medium (n=6), 40µg/ml Fibronectin (n=5), or 10µg/ml Collagen 1 (n= 5). Bar: 10µm. *(I)* Representative images of SK2/Sig-1R and p-AKT-S473 staining in PDAC patient samples. Arrows highlight cells where SK2/Sig-1R colocalize with p-AKT. Scale bar 50 µm**.** (*P< 0,05, **P< 0,01; ***P< 0,001; ns: not significant).

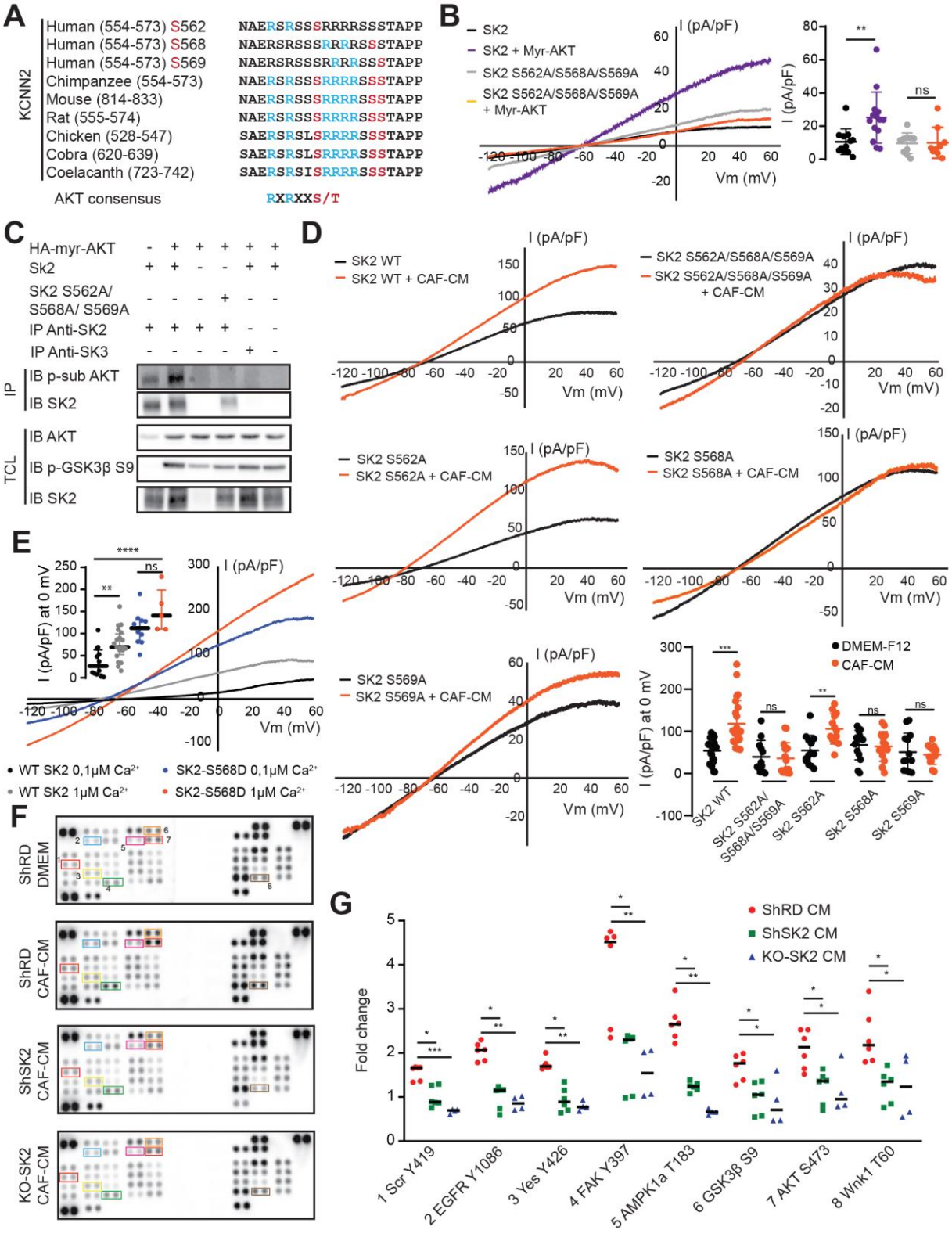

Figure 4: SK2 is a pivotal regulator of AKT signaling. *(A)* Sequence alignment of the AKT phosphorylation consensus site within SK2 orthologs from different species. *(B)* Patch clamp recording of ISK2 in HEK293 expressing either wild type SK2 alone (n=12), wild type SK2 with a HA-Myr-AKT construct (n= 14), SK2 carrying a triple mutation (S562A, S568A, S569A) alone

(n=10) or SK2 carrying the triple mutation with a HA-Myr-AKT construct (n=9). *(C)* Immunoblot (IB) of total cell lysate (TCL) and immunoprecipitants (IP) from HEK293 cells transfected with SK2 WT or SK2 carrying the triple mutation and HA-Myr-Akt construct as indicated. The protein precipitation has been done with SK2 antibody (or SK3 antibody: negative control) and revealed with a p-AKT substrate (RXRXXpS/pT) antibody, n=3. *(D)* Patch clamp recording of SK2 currents recorded in HEK293 cells transfected with WT SK2 (Ctl n=24; CAF-CM, n=24), SK2 carrying the triple mutations (Ctl n=12; CAF-CM, n=16), or SK2 carrying each single mutation S562A (Ctl n=13; CAF-CM, n=13), S568A, (Ctl n=14; CAF-CM, n=14) and S569A (Ctl n=13; CAF-CM, n=13) treated overnight with control medium (black) or CAF-CM (red). *(E)* Patch clamp recording of SK2 currents in HEK293 cells transfected with WT SK2 or SK2 carrying the mutation S568D and exposed to two different concentrations of extracellular Ca^{2+}, 1µM and 100nM (WT SK2 100nM, n=12; WT SK2 1µM, n= 20; S568D 100nM, n=10; S568D 1µM, n=5). *(F)* Representative images showing the phospho-kinase array for ShRD PANC-1 cells exposed to control medium (DMEM/F12) or CAF-CM, and from ShSK2 or KO-SK2 PANC-1 cells exposed to CAF-CM. Each kinase is spotted in duplicate and the location of EGFR, Akt (S473), Yes, Src, FAK, GSK3, AMPK, and Wnk1 is indicated using colored boxes. *(G)* Quantitative analysis of the spots from *(F)* was performed by densitometry and presented as fold change vs. control cells. Experiments were performed in experimental duplicates (n=3). (*P< 0,05, **P< 0,01; ***P< 0,001; ****P<0.0001 ns: not significant).

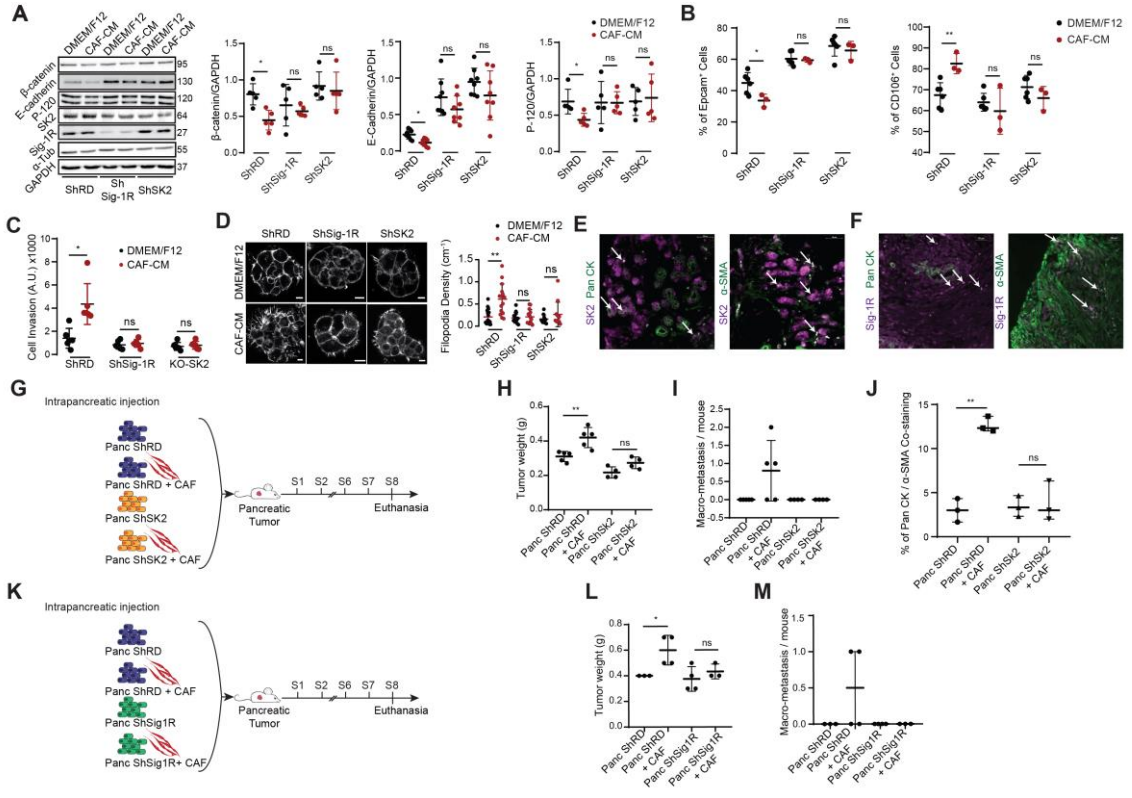

Figure 5: SK2 drives PCC aggressiveness in response to CAF secretome. *(A)* Western blot analysis showing the protein expression of adherens junction markers in ShRD; ShSig-1R, or ShSK2 PANC-1 cells, exposed overnight to control medium (DMEM/F12) or CAF-CM. Densitometric quantifications are shown as scatter plots, (E-cadherin (n=9); β-catenin (n=5); p-120 catenin (n=5); Sig-1R (n=4) and SK2 (n=8)). *(B)* Graphs showing the percentage of cells positive for Epcam (left panel) or CD106 (right panel) markers in Sh-RD, ShSig-1R and ShSK2 challenged with control (DMEM/F12) or CAF-CM (CAF-CM). Labelling was quantified by FACS (n=3, *P< 0,05). *C)* ShRD, ShSig-1R and ShSk2 PANC-1 cells were treated with control medium or CAF-CM and subjected to cell invasion assay (n=5 *P<0,05). *(D)* Confocal immunofluorescence images from ShRD; ShSig-1R and ShSK2 PANC-1 cells, grown in Matrigel (3D cell culture) showing F-actin staining. The scatter plot represents data dispersion and median values of Filopodia density (ShRD DMEM/F12 (n=18); ShRD CAF-CM (n=15); ShSig-1R DMEM/F12 (n=13); ShSig-1R CAF-CM (n=13); ShSK2 (n=11); ShSK2 CAF-CM (n=12)). Scale bar:10µm. *(E)* Representative immunofluorescence images of SK2 (magenta), Pan CK (green, left panel) or α-SMA (green, right panel) in PDAC-patient samples. Scale Bar

50µm. *(F)* Representative immunofluorescence images of Sig-1R (magenta) Pan CK (green, left panel) or α-SMA (green, right panel) in PDAC-patient samples. Scale Bar 50µm. *(G)* Graphical scheme explaining the experimental workflow for *(H-J)*. *(H)* Graph showing pancreatic tumor weight of PANC ShRD (n=5), PANC ShRD + CAF (n=5), PANC ShSK2 (n=4) and PANC ShSK2 + CAF (n=4), 8 weeks after orthotopic injection. Corresponding counted liver macro metastasis per mouse are presented in (*I*). *(J)* Corresponding graphs showing the percentage of Pan CK labelled cells positive for α-SMA staining (n= 3, each). *(K)* Graphical scheme explaining the experimental workflow for (L, M). *(L)* (Graph showing pancreatic tumor weight of PANC-1 ShRD (n=3), PANC-1 ShRD + CAF (n=4), PANC-1 ShSig-1R (n=4) and PANC-1 ShSig-1R + CAF (n=3), 8 weeks after orthotopic injection. Corresponding counted liver macro metastasis per mouse are presented in *(M).* Analysis of variance (ANOVA) was used for statistical analysis. (*P< 0,05, **P< 0,01; ns: not significant).

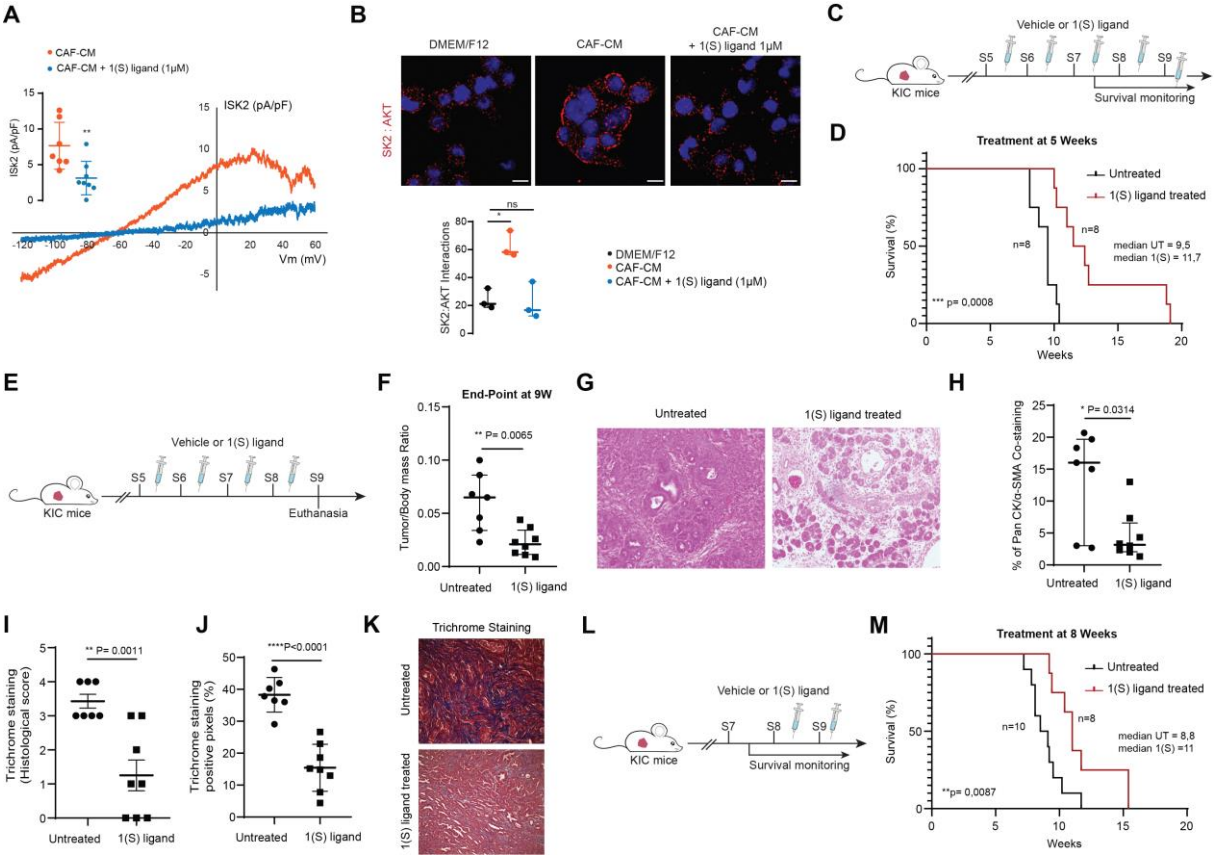

Figure 6: Sig-1R ligand 1(S) inhibits SK2 activity and reduces CAF secretome-induced aggressiveness. *(A)* Patch clamp recording of ISK2 in PANC-1 cells exposed to CAF-CM (n=7) or CAF-CM + 1(S) ligand (1µM; n=8) overnight. *(B)* PLA analysis of SK2/AKT interaction in ShRD PANC-1 cells, treated with control medium, CAF-CM or CAF-CM + 1(S) ligand (1µM; n=3) overnight. Bar, 10µm. *(C)* Graphical scheme describing the KIC mice treatment workflow. KIC mice were injected at 5 weeks with vehicle or 1(S) ligand treatments, once a week until each animal reached clinical endpoint. *(D)* Kaplan-Meier survival of KIC mice treated with vehicle (n=8) or 1(S) ligand (n=8) from 5 weeks old. *(E)* Graphical scheme describing the KIC mice treatment workflow. KIC mice were injected at 5 weeks with vehicle or 1(S) ligand treatment, once a week until the animals were euthanized at 9 weeks old. *(F)* Graphs showing pancreatic tumor mass over body mass ratio at end-point of 9 weeks for KIC mice treated with vehicle (n=7) or 1(S) ligand (n=8). *(G)* Representative pictures of H&E staining of KIC mice pancreatic tumors treated with vehicle or 1(S) ligand. *(H)* Graphs showing the percentage of Pan CK labelled cells positive for α-SMA staining in control (untreated, n= 7) and 1(S) ligand-treated mice (1(S) ligand, n= 8). *(I)* Graphs showing the histological score of trichrome labelling in control (untreated, n= 7) and 1(S) ligand-treated mice (1(S) ligand, n= 8). *(J)* Graphs showing the percentage of trichrome staining positive pixels in control (untreated, n= 7) and 1(S) ligand-treated mice (1(S) ligand, n= 8). *(K)* Corresponding micrographs showing representative trichrome labelling in control (Untreated) and treated animals (1(S) ligand treated). *(L)* Graphical scheme describing the KIC mice treatment workflow. KIC mice were injected at 8 weeks with vehicle or 1(S) ligand treatment, once a week until each animal reached clinical endpoint. *(M)* Kaplan-Meier survival of KIC mice treated with vehicle (n=10) or 1(S) ligand (n=8) from 8 weeks old. (*P< 0,05, **P< 0,01, ***< 0.001; ns: not significant).

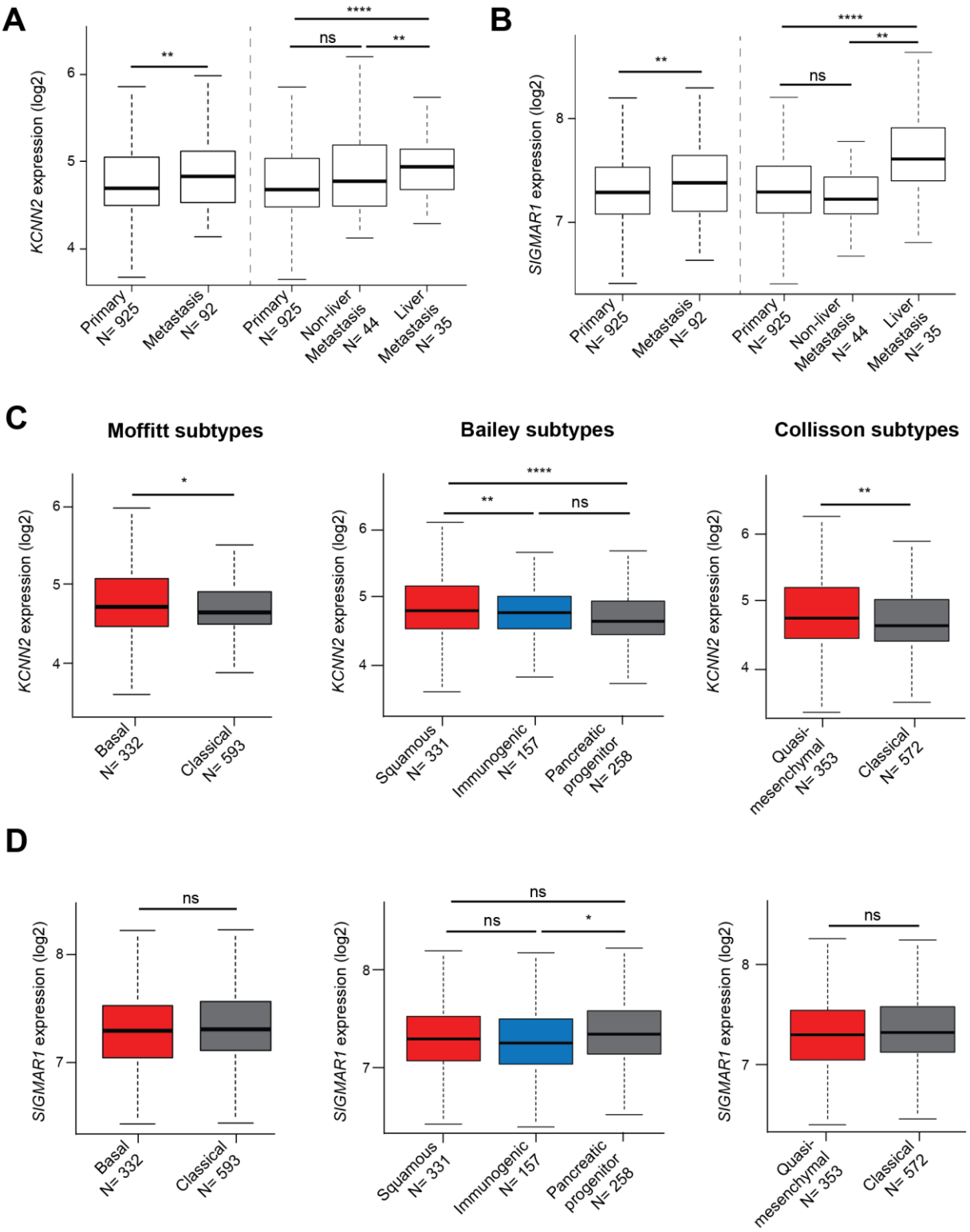

Figure 7: Gene expression of KCNN2 and SIGMAR1 in clinical PDAC samples. *(A)* Box plots of and *KCNN2 (B) SIGMAR1* expression (log2) in primary cancers *versus* metastases, and in liver metastases *versus* non-liver metastases. *(C)* Box plots of *KCNN2* and *(D) SIGMAR1* expression (log2) in primary cancers according to the molecular PDAC subtypes

identified by Moffit et al. (left), Bailey et al. (middle), and Collisson et al (right). For each box plot, median and ranges are indicated. Student t-test *p<0.05; **p<0.01; ***p<0.001; ****p<0.0001; ns: not significant. As shown in Table S4, these results remained similar and significant after adjustment for the estimated tumor cellularity (ESTIMATE algorithm, R-library, version 1.0.13), for both SIGMAR1 and KCNN2.

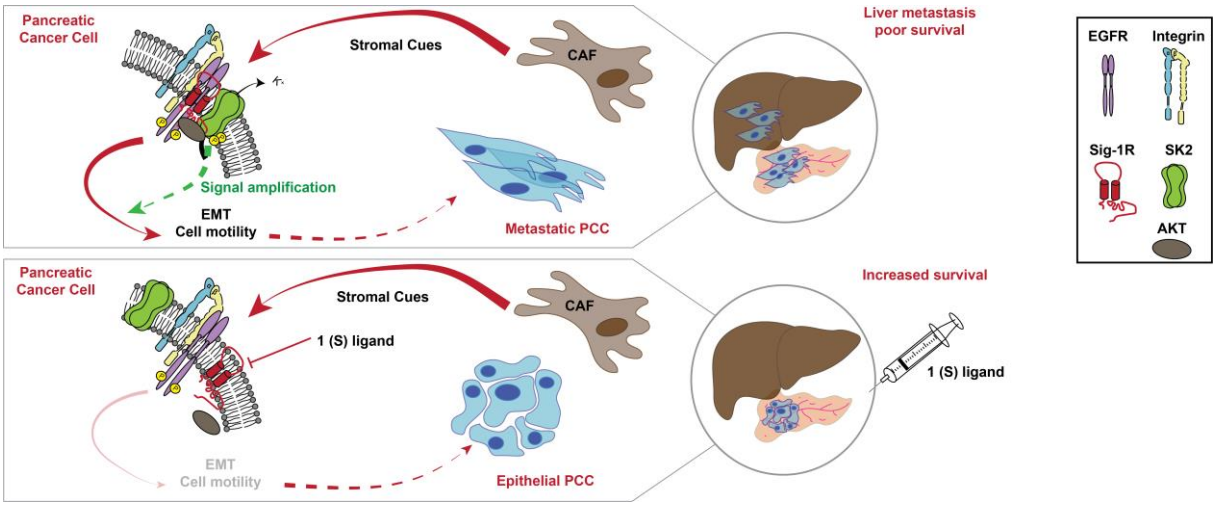

Figure 8: Schematic diagram showing the mechanism by which CAF-secretome activate a SK2 dependent β-1-integrin-EGFR-AKT signaling hub that promotes PCC aggressiveness. This mechanism can be pharmacologically targeted through Sig1-R to counteract the intercellular communication between CAF and PCC in PDAC.

References:

1. Neesse A, Bauer CA, Öhlund D, et al. Stromal biology and therapy in pancreatic cancer: ready for clinical translation? Gut 2019;68:159-171.
2. Schnittert J, Bansal R, Prakash J. Targeting Pancreatic Stellate Cells in Cancer. Trends Cancer 2019;5:128-142.
3. Leca J, Martinez S, Lac S, et al. Cancer-associated fibroblast-derived annexin A6+ extracellular vesicles support pancreatic cancer aggressiveness. J Clin Invest 2016;126:4140-4156.
4. Hwang RF, Moore T, Arumugam T, et al. Cancer-associated stromal fibroblasts promote pancreatic tumor progression. Cancer Res 2008;68:918-26.
5. Özdemir BC, Pentcheva-Hoang T, Carstens JL, et al. Depletion of carcinoma-associated fibroblasts and fibrosis induces immunosuppression and accelerates pancreas cancer with reduced survival. Cancer Cell 2014;25:719-34.
6. Rhim AD, Oberstein PE, Thomas DH, et al. Stromal elements act to restrain, rather than support, pancreatic ductal adenocarcinoma. Cancer Cell 2014;25:735-47.

7. Shi Y, Gao W, Lytle NK, et al. Targeting LIF-mediated paracrine interaction for pancreatic cancer therapy and monitoring. Nature 2019;569:131-135.
8. Auciello FR, Bulusu V, Oon C, et al. A Stromal Lysolipid-Autotaxin Signaling Axis Promotes Pancreatic Tumor Progression. Cancer Discov 2019;9:617-627.
9. Kourrich S, Su TP, Fujimoto M, et al. The sigma-1 receptor: roles in neuronal plasticity and disease. Trends Neurosci 2012;35:762-71.
10. Kourrich S, Hayashi T, Chuang JY, et al. Dynamic interaction between sigma-1 receptor and Kv1.2 shapes neuronal and behavioral responses to cocaine. Cell 2013;152:236-47.
11. Tsai SY, Hayashi T, Mori T, et al. Sigma-1 receptor chaperones and diseases. Cent.Nerv.Syst.Agents Med.Chem. 2009;9:184-189.
12. Song L, Bekdash R, Morikawa K, et al. Sigma non-opioid receptor 1 is a potential therapeutic target for long QT syndrome. *Nat Cardiovasc Res* 2022;1:142–156.
13. Gueguinou M, Crottès D, Chantôme A, et al. The SigmaR1 chaperone drives breast and colorectal cancer cell migration by tuning SK3-dependent Ca. Oncogene 2017;36:3640-3647.
14. Crottès D, Rapetti-Mauss R, Alcaraz-Perez F, et al. SIGMAR1 Regulates Membrane Electrical Activity in Response to Extracellular Matrix Stimulation to Drive Cancer Cell Invasiveness. Cancer Res 2016;76:607-18.
15. Prevarskaya N, Skryma R, Shuba Y. Ion Channels in Cancer: Are Cancer Hallmarks Oncochannelopathies? Physiol Rev 2018;98:559-621.
16. Pardo LA, Stuhmer W. The roles of K(+) channels in cancer. Nat Rev Cancer 2014;14:39-48.
17. Crottès D, Lin YT, Peters CJ, et al. TMEM16A controls EGF-induced calcium signaling implicated in pancreatic cancer prognosis. Proc Natl Acad Sci U S A 2019;116:13026-13035.
18. Renaudo A, L'Hoste S, Guizouarn H, et al. Cancer cell cycle modulated by a functional coupling between sigma-1 receptors and Cl- channels. Journal of biological chemistry 2007;282:2259-2267.
19. Rapetti-Mauss R, Bustos V, Thomas W, et al. Bidirectional KCNQ1:β-catenin interaction drives colorectal cancer cell differentiation. Proc Natl Acad Sci U S A 2017;114:4159-4164.
20. Zhou Y, Wong CO, Cho KJ, et al. SIGNAL TRANSDUCTION. Membrane potential modulates plasma membrane phospholipid dynamics and K-Ras signaling. Science 2015;349:873-6.
21. Crottès D, Martial S, Rapetti-Mauss R, et al. Sig1R protein regulates hERG channel expression through a post-translational mechanism in leukemic cells. J Biol Chem 2011;286:27947-58.
22. Balasuriya D, Stewart AP, Crottès D, et al. The sigma-1 receptor binds to the Nav1.5 voltage-gated Na+ channel with 4-fold symmetry. J Biol Chem 2012;287:37021-9.
23. Jiang H, Hegde S, Knolhoff BL, et al. Targeting focal adhesion kinase renders pancreatic cancers responsive to checkpoint immunotherapy. Nat Med 2016;22:851-60.
24. Grzesiak JJ, Bouvet M. The alpha2beta1 integrin mediates the malignant phenotype on type I collagen in pancreatic cancer cell lines. Br J Cancer 2006;94:1311-9.
25. Zaghdoudi S, Decaup E, Belhabib I, et al. FAK activity in cancer-associated fibroblasts is a prognostic marker and a druggable key metastatic player in pancreatic cancer. EMBO Mol Med 2020;12:e12010.
26. Ricono JM, Huang M, Barnes LA, et al. Specific cross-talk between epidermal growth factor receptor and integrin alphavbeta5 promotes carcinoma cell invasion and metastasis. Cancer Res 2009;69:1383-91.
27. Rhim AD, Mirek ET, Aiello NM, et al. EMT and dissemination precede pancreatic tumor formation. Cell 2012;148:349-61.
28. Pastushenko I, Brisebarre A, Sifrim A, et al. Identification of the tumour transition states occurring during EMT. Nature 2018;556:463-468.
[Dataset] 29. Stratford JK, Bentrem DJ, Anderson JM, et al. Data from : A six-gene signature predicts survival of patients with localized pancreatic ductal adenocarcinoma. PLoS Med 2010;7:e1000307. Gene Expression Omnibus https://doi.org/10.1371/journal.pmed.1000307

30. Fiori ME, Di Franco S, Villanova L, et al. Cancer-associated fibroblasts as abettors of tumor progression at the crossroads of EMT and therapy resistance. Mol Cancer 2019;18:70.
31. Oxombre B, Lee-Chang C, Duhamel A, et al. High-affinity σ1 protein agonist reduces clinical and pathological signs of experimental autoimmune encephalomyelitis. Br J Pharmacol 2015;172:1769-82.
32. Collignon A, Silvy F, Robert S, et al. Dendritic cell-based vaccination: powerful resources of immature dendritic cells against pancreatic adenocarcinoma. Oncoimmunology 2018;7:e1504727.
[Dataset] 33. Bailey P, Chang DK, Nones K, et al. Data from : Genomic analyses identify molecular subtypes of pancreatic cancer. Nature 2016;531:47-52. European Genome-phenome Archive https://doi.org/10.1038/nature16965
[Dataset] 34. Collisson EA, Sadanandam A, Olson P, et al. Data from : Subtypes of pancreatic ductal adenocarcinoma and their differing responses to therapy. Nat Med 2011;17:500-3. Gene Expression Omnibus https://doi.org/10.1038/nm.2344
[Dataset] 35. Moffitt RA, Marayati R, Flate EL, et al. Data from : Virtual microdissection identifies distinct tumor- and stroma-specific subtypes of pancreatic ductal adenocarcinoma. Nat Genet 2015;47:1168-78. Gene Expression Omnibus https://doi.org/10.1038/ng.3398
36. Provenzano PP, Cuevas C, Chang AE, et al. Enzymatic targeting of the stroma ablates physical barriers to treatment of pancreatic ductal adenocarcinoma. Cancer Cell 2012;21:418-29.
37. Chen Y, Kim J, Yang S, et al. Type I collagen deletion in αSMA. Cancer Cell 2021;39:548-565.e6.
38. Ligorio M, Sil S, Malagon-Lopez J, et al. Stromal Microenvironment Shapes the Intratumoral Architecture of Pancreatic Cancer. Cell 2019;178:160-175.e27.
39. Jiang SH, Zhu LL, Zhang M, et al. GABRP regulates chemokine signalling, macrophage recruitment and tumour progression in pancreatic cancer through tuning KCNN4-mediated Ca. Gut 2019.
40. Samain R, Brunel A, Douché T, et al. Pharmacologic Normalization of Pancreatic Cancer-Associated Fibroblast Secretome Impairs Prometastatic Cross-Talk With Macrophages. Cell Mol Gastroenterol Hepatol 2021;11:1405-1436.
41. Jagadeeshan S, Krishnamoorthy YR, Singhal M, et al. Transcriptional regulation of fibronectin by p21-activated kinase-1 modulates pancreatic tumorigenesis. Oncogene 2015;34:455-64.
42. Kim YJ, Jung K, Baek DS, et al. Co-targeting of EGF receptor and neuropilin-1 overcomes cetuximab resistance in pancreatic ductal adenocarcinoma with integrin β1-driven Src-Akt bypass signaling. Oncogene 2017;36:2543-2552.
43. Navas C, Hernández-Porras I, Schuhmacher AJ, et al. EGF receptor signaling is essential for k-ras oncogene-driven pancreatic ductal adenocarcinoma. Cancer Cell 2012;22:318-30.
44. Ardito CM, Grüner BM, Takeuchi KK, et al. EGF receptor is required for KRAS-induced pancreatic tumorigenesis. Cancer Cell 2012;22:304-17.
45. Rodríguez-Muñoz M, Cortés-Montero E, Pozo-Rodrigálvarez A, et al. The ON:OFF switch, σ1R-HINT1 protein, controls GPCR-NMDA receptor cross-regulation: implications in neurological disorders. Oncotarget 2015;6:35458-77.
46. Abatematteo FS, Niso M, Contino M, et al. Multi-Target Directed Ligands (MTDLs) Binding the σ. Int J Mol Sci 2021;22.
47. Chu UB, Ruoho AE. Biochemical Pharmacology of the Sigma-1 Receptor. Mol Pharmacol 2016;89:142-53.